G.M. CARMEL VIGILA BAI,[1] R. ABISHA[2, 3]

[1] Department of Physics, Government Arts and Science College
   (Konam, Nagercoil-629 004, Tamilnadu, India; e-mail: gmcarmelvb@gmail.com)
[2] Department of Physics, Rani Anna Government College for Women
   (Tirunelveli-08, Tamilnadu, India; e-mail: abisharusselraj@gmail.com)
[3] Affiliated to Manonmaniam Sundaranar University, Abhishekapatti
   (Tirunelveli-12, Tamilnadu, India)

POSSIBLE 2p DECAY EMISSION IN THE REGION $4 \leq Z \leq 54$ USING THE MODIFIED CYE MODEL

Two proton radioactivity is the spontaneous emission of two protons simultaneously from the nucleus. We have extended our CYE model to study this 2p radioactivity. The current work aims to study the 2p radioactivity of nuclei between $Z \geq 4$ to $Z \leq 54$. Moreover, the impact of a deformation of the nucleus is also examined. To comprehend two-proton decay, numerous theoretical works have been developed. The half lifetimes for 2p decays calculated using this CYE model are in a good accord with CPPMDN model of K.P. Santhosh, GLDM, ELDM, GLM, Sreeja et al. and Liu et al. and SEB, SHF and UFM. From whence, it appears that the CYE model is a reasonable choice for assessing 2p radioactivity.

K e y w o r d s: 2p radioactivity, CYE model, half lifetime, deformation effects.

1. Introduction

Two proton (2p) radioactivity is the simultaneous emission of two protons from a nuclear ground state near or beyond proton drip line with a measurable half lifetime. The 2p radioactivity phenomenon may occur due to the effect of proton pairing, when even proton number (even $-Z$) nuclei lying near the proton drip line. Zel'dovich made the initial discovery of two-proton (2p) radioactivity in the 1960s [1], and Goldansky later described the mechanism [2]. In 1978, the diproton correlation was carried out for the 2p decay of ^{12}O. Based on its nuclear binding energy, it was assumed to be a diproton emitter. The ^{16}Ne isotope has been under-researched for a very long time. It was additionally considered to be a diproton emitter based on its nuclear binding energy [3]. The first experimental attempts to access isotopes of light 2p unbound nuclei near the proton drip line was carried out in 1984 [4]. In 1991, two protons could be consideredgether as one quasi-particle "diproton" with charge 2 and mass 2 [5]. In 1996, the research was conducted on the 2p decay of the excited ^{14}O nucleus brought about by the resonance reaction ^{13}N + p [6]. The first excited state 3/2 in ^{17}Ne is an intriguing candidate for the 2p decay. Experimental attempts to study this state were made several times [7]. Mukha *et al.* devised a novel method for studying the 2p decay. In 2001, IT WAs complementary to implantation approaches in gases and solids and is ideally adapted for the in-flight investigation of very short-lived 2p emitters [8]. Following more than 40 years of study, the f 2p emitter was ultimately identified in the decay of ^{45}Fe in 2002 [9, 10]. Since then, numerous additional theoretical and experimental investigations of this phenomena WERe advanced. In addition, the GANIL group discovered ^{54}Zn [11], another 2p-emitting isotope. Mukha *et al.* [12] found another intriguing example of 2p radioactivity from thE high-lying 21+ isomer in ^{94}Ag in 2006. In 2006, Rotureau *et al.* [13] studied two-proton radioactivity in the framework of the shell model embedded in the continuum. The two-proton radioactivity wss treated

as a two-body problem in which the valance protons sre emitted as a cluster. As a result, the three-body asymptotic behavior is violated, and the detailed information for the configurations of the valence protons is largely lost. The innovative work used to explore the two-proton radioactivity for ^{19}Mg'swas reported in 2007 [14]. Using silicon microstrip detectors, the in-flight decay approach carefully reconstructs the paths of all decay products. In 2007–2008 with the aid of gaseous time-projection chambers, it was possible to observe the 2p radioactivity directly and to study the p–p correlation (TPC). Those detectors enable the recording of proton track projections on the TPC's anode plane, thereby validating the ^{45}Fe decay's 2p emission [15]. The individual 2p decay events for ^{45}Fe were then captured on camera using a novel optical TPC detector (OTPC) [16]. The ^{16}Ne isotope was researched by Mukha *et al.* in 2008 utilizing the newly established the in-flight decay technology [17]. On the basis of the hyper-spherical harmonics approach, Grigorenko [18] studied two-proton radioactivity as a three-body (core + p + p) problem in 2009 and, In 2010, another proton emitter, ^{8}C. This isotope was thought to decay through the simultaneous release of four protons. Using the invariant mass approach, the 2p decays of the ^{12}O [19] and ^{16}Ne [20] were experimentally studied. Eventually, in 2016, the French group at the fragment separator Big RIPS in RIKEN [21] observed the fourth 2p emitter, ^{67}Kr with a half-lifetime of a few milliseconds. Another 2p-unbound isotope ^{11}O has been discovered in 2019 [22]. The novel 2p-emitting isotopes ^{29,30}Ar and the FRS will be tested in a pilot experiment in 2019. Several authors have published numerous papers utilizing various theoretical frameworks that describe 2p radioactivity as a ^{2}He cluster decay process. A number of theoretical models such as the effective liquid drop model (ELDM) [23], empirical formulas were proposed by sreeja *et al.* [24], generalized liquid drop model (GLDM) [25], Gamow like model (GLM) [26], Coulomb and proximity potential model, for deformed nuclei (CPPMDN) by K.P. Santhosh [27], and New Geiger–Nuttall Law by Liu *et al.* [28] to analyze 2p radioactivity and half lifetimes of the 2p radioactivity from 2006. Through these methods, the experimental 2p radioactivity half lifetimes have also been successfully replicated in several authenticity.

In our earlier research, we explored the alpha decay, cluster decay, and spontaneous fission decay charac-

teristics of Actinide, Transactinide and superheavy nuclei with and without adding deformation effects using the CYE model [29–34]. In this study, the Cubic Plus Yukawa Plus Exponential Model (CYE) was modified to comprehensively examine the half lifetimes of two proton radioactivity using the concept of that the proton pairing interaction and the odd-even binding energy effect $Z = 2m + 2$. This model is useful for analyzing double proton decay from a variety of proton-rich nuclei. In our early work, we calculated the half lifetime of 2p decay for $Z \geq 4$ to $Z \leq 36$ [35] and $Z \geq 4$ to $Z \leq 54$ [36] and Super heavy mass region $Z \geq 100$ to $Z \leq 111$ [37].

2. Cubic Plus Yukawa Plus Exponential (CYE) Model

In the ongoing work, we used a realistic model [38], known as the CYE model, to examine the decay properties. In this model, a cubic potential in the pre-scission zone is connected to the Coulomb plus Yukawa plus Exponential potential in the post-scission region. Without going against the principle of energy conservation, the zero-point vibration energy is expressly incorporated here. The proton pairs are already present in the nucleus at a specific distance from the nucleus, and the proton particle only encounters pure coulomb potential. This potential as a function of r which is the center of mass distance of the two fragments for the post scission region is given by,

$$V(r) = \frac{Z_1 Z_2\, e^2}{r} + V_n(r) - Q; \quad r \geq r_t, \qquad (1)$$

where, $V_n(r)$ is the nuclear interaction energy and written in the form

$$V_n(r) = -D\left[F + \frac{r - r_t}{a}\right]\frac{r_t}{r}\exp\left[\frac{r_t - r}{a}\right].$$

Using the relation, the system's half-lifetime is estimated as

$$T = \frac{1.433 \times 10^{-21}}{E_v}[1 + \exp(K)], \qquad (2)$$

where

$$K = \frac{2}{\hbar}\int_{r_a}^{r_t}[2B_r(r)\,V(r)]^{1/2}\,dr +$$

$$+ \frac{2}{\hbar}\int_{r_t}^{r_b}[2B_r(r)\,V(r)]^{1/2}\,dr.$$

Here, r_a and r_b are the two appropriate zeros of the integrand.

3. Potential for the Post-Scission Region

The parent and daughter nuclei are regarded as spheroids in this work. If the ejected nucleus is spherical and the daughter nucleus only exhibits a single deformation, such as a quadruple deformation, and if the reaction's Q value is assumed to be the origin, then the potential for the post-scission is given by

$$V\left(r\right) = V_c\left(r\right) + V_n\left(r\right) - V_{df}\left(r\right) - Q; \quad r \geq r_t. \tag{3}$$

Here, $V_c(r)$ is the Coulomb potential between a spheroidal daughter and spherical emitted fragment, $V_n(r)$ is the nuclear interaction energy due to finite range effects, $V_{df}(r)$ is a change in the nuclear interaction energy due to quadruple deformation (β_2) of the daughter nucleus

For a prolate spheroid daughter nucleus with longer axis along the fission direction,

$$V_c\left(r\right) = \frac{3}{2}\frac{Z_1 Z_2\, e^2 \gamma}{r}\left[\frac{1-\gamma^2}{2}\ln\frac{\gamma+1}{\gamma-1} + \gamma\right]. \tag{4}$$

For an oblate spheroid daughter with shorter axis along the fission direction

$$V_c\left(r\right) = \frac{3}{2}\frac{Z_1 Z_2\, e^2}{r}\left[\gamma\left(1+\gamma^2\right)\arctan\gamma^{-1} - \gamma^2\right]. \tag{5}$$

Here,
$$\gamma = \frac{r}{\left(a_2^2 - b_2^2\right)^{1/2}}.$$

Here, a_2 and b_2 are the semimajor and minor axes of the spheroidal daughter nucleus, respectively.

If the nuclei have spheroid shape, the radius vector $R\left(\theta\right)$ making an angle θ with the axis of symmetry locating sharp surface of a deformed nuclei is given by

$$R\left(\theta\right) = R_0\left[1 + \sum_{n=0}^{\infty}\sum_{m=-n}^{n}\beta_{nm}Y_{nm}(\theta)\right]. \tag{6}$$

Here, R_0 is the radius of the equivalent spherical nucleus.

The Change in the nuclear interaction energy due to the quadruple deformation β_2 of the daughter nucleus is given by

$$V_d = \frac{4R_2^3 C_s A_2 \beta_2}{a r_0^2}\left(\frac{5}{4\pi}\right)^{1/2}.$$

4. Potential for the PRE-scission region

A third order polynomial in r provides an approximation of the potential barrier's shape in the overlapped region between the ground state and the contact point

$$V(r) = -E_v + \left[V\left(r_t\right) + E_v\right]\left\{s_1\left[\frac{r-r_i}{r_t-r_i}\right]^2 - s_2\left[\frac{r-r_i}{r_t-r_i}\right]^3\right\}; \quad r_i \leq r \leq r_t, \tag{7}$$

where r_i is the distance between the centers of mass of two portions of the daughter and the emitted nuclei in the spheroidal parent nucleus and $r_t = a_2 + R_1$. Here, a_2 is the semi major or minor axis of the spheroidal daughter nucleus depending on the shape.

If we consider spheroid deformation β_2, then

$$R\left(\theta\right) = R_0\left[1 + \beta_2\left(\frac{5}{4\pi}\right)^{1/2}\left(\frac{3}{2}\cos^2\theta - \frac{1}{2}\right)\right] \tag{8}$$

and if the Nilsson's hexadecapole deformation β_4 is also included in the deformation, then Eq. (6) becomes

$$R\left(\theta\right) = R_0\left[1 + \beta_2\left(\frac{5}{4\pi}\right)^{1/2}\left(\frac{3}{2}\cos^2\theta - \frac{1}{2}\right) + \right.$$
$$\left. + \beta_4\left(\frac{9}{4\pi}\right)^{1/2}\frac{1}{8}\left(35\cos^4\theta - 30\cos^2\theta + 3\right)\right]. \tag{9}$$

For calculating the zero point vibration energy E_v,

$$E_v = \frac{\pi\hbar}{2}\left[\frac{\left(\frac{2Q}{\mu}\right)^{1/2}}{(C_1 + C_2)}\right],$$

C_1 and C_2 are the central radii of the fragments given by

$$C_i = 1.18\, A^{1/3} - 0.48 \quad (i = 1, 2)$$

and reduced mass,

$$\mu = \frac{m_1 m_2}{m_1 + m_2}.$$

5. Result and Disscussion

In this work, we have executed assessments on the two-proton (2p) radioactivity half lifetimes of ^{6}Be, ^{12}O, ^{16}Ne, ^{19}Mg, ^{45}Fe, ^{48}Ni, ^{54}Zn and ^{67}Kr by using CYE model by incorporating the modification for

Table 1. **Comparison between the predicted half lifetimes**
by using CPPMDN, GLDM, ELDM, GLM, two empirical formulas
and the experimental one with yje modified CYE odel without including deformation

Parent nuclei	Q_{2p} (MeV)	Log$_{10} T_{1/2}(s)$										
		CPPMDN [27]	GLDM [25]	ELDM [23]	GLM [26]	EF [24]	GNL [28]	SEB [39]	SHF [40]	UFM [41]	Exp. values	CYEM calculated
^{6}Be	1.372 [42]	−21.91	−19.37	−19.97	−19.7	−21.95	−23.81	−19.41	−	−19.41	$−20.30^{+0.03}_{-0.03}$ [42]	−21.41
^{12}O	1.638 [19]	−20.9	−19.17	−18.27	−18.04	−18.47	−20.17	−17.70	−	−18.45	>20.20 [19]	−15.81
^{16}Ne	1.401 [43]	−18.25	−16.63	−16.6	−16.43	−16.16	−17.77	−15.71	−	−16.68	$−20.38^{+0.03}_{-0.03}$ [43]	−14.47
^{19}Mg	0.750 [14]	−11.96	−11.79	−11.72	−11.46	−10.66	−12.03	−10.58	−	−11.77	$−11.40^{+0.14}_{-0.20}$ [14]	−10.25
^{45}Fe	1.100 [9]	−2.76	−2.23	−	−2.09	−1.81	−2.21	−2.32	−2.31	−1.94	$−2.40^{+0.26}_{-0.26}$ [9]	−1.94
^{48}Ni	1.290 [44]	−2.17	−2.62	−	−2.59	−1.61	−2.59	−2.55	−2.23	−2.29	$−2.52^{+0.24}_{-0.22}$ [44]	−1.67
^{54}Zn	1.280 [45]	−1.45	−0.87	−	−0.93	−0.1	−0.93	−1.31	−1.32	−0.52	$−2.76^{+0.15}_{-0.14}$ [45]	−0.9
^{67}Kr	1.690 [21]	−1.06	−1.25	−0.06	−0.76	0.31	−0.58	−0.95	−1.05	−0.54	$−1.70^{+0.02}_{-0.02}$ [21]	0.11

Table 2. **Comparison between the predicted half lifetimes**
by using CPPMDN and the experimental one with CYE model
with including deformation. The values of deformation are taken by Möller *et al.* [46]

Parent nuclei	Q_{2p} (MeV)	Log $_{10}T_{1/2}(s)$			
		CPPMDN [27]	Experimental value (9, 10)	CYE model (without deformation)	CYE model (with deformation $\beta_2 P \beta_2 D$)
$^{45}_{26}$Fe	1.100 [9]	$−2.76^{+0.30}_{-0.30}$	$−2.40^{+0.26}_{-0.26}$	−1.94	−1.974
	1.140 [10]	$−2.36^{+0.59}_{-0.63}$	$−2.07^{+0.24}_{-0.21}$	−1.91	−2.989
	1.154 [46]	$−2.53^{+0.19}_{-0.19}$	$−2.55^{+0.13}_{-0.12}$	−1.96	−2.856
	1.210 [47]	$−3.15^{+0.57}_{-0.55}$	$−2.42^{+0.03}_{-0.03}$	−2.10	−2.970
$^{48}_{28}$Ni	1.290 [44]	$−2.17^{+0.43}_{-0.45}$	$−2.52^{+0.24}_{-0.22}$	−1.67	−0.322
	1.350 [46]	$−2.79^{+0.20}_{-0.21}$	$−2.08^{+0.40}_{-0.78}$	−2.00	−0.909
	1.310 [48]	$−2.38^{+0.42}_{-0.45}$	$−2.52^{+0.24}_{-0.22}$	−1.77	−0.098
$^{54}_{30}$Zn	1.280 [45]	$−1.45^{+0.07}_{-0.07}$	$−2.76^{+0.15}_{-0.14}$	−0.90	−0.358
	1.480 [11]	$−2.59^{+0.19}_{-0.19}$	$−2.43^{+0.20}_{-0.14}$	−1.65	−1.301
$^{67}_{36}$Kr	1.690 [21]	$−1.06^{+0.16}_{-0.16}$	$−1.70^{+0.02}_{-0.02}$	0.11	−0.426

two proton radioactivity. In Tables 1–4, we compare the theoretical predictions with one another. In Table 1, the table's first, second, and third columns, respectively, list the nuclei that show 2p radioactivity, experimental Q_{2p} values, and experimental half lifetimes. Without accounting for deformation effects, our CYE model half lifetime values are compared with other models of ELDM [23], Sreeja *et al.* [24], GLDM [25], GLM [26], CPPMDN by K.P. Santhosh [27], and Liu *et al.* [28] and SEB [39], SHF [40] and UFM [41] with experimental values column 4–13. The Q values for the reaction are acquired from the reference [25, 39] and the experimental values from reference [9, 10]. The comparison reveals that the attained values are well coinciding with other anticipated values.

Table 3. **Comparison between the predicted even *Z*-nuclei half-lives by using CPPMDN, GLDM, ELDM, GLM, two empirical formulas SEB and SHF the experimental one with Modified CYEM with and without including deformation. The experimental Q_{2p} values are taken from the references [23]. The values of deformation are taken by Möller *et al.* [49]**

Parent nuclei	Q_{2p} (MeV) [23]	$\mathrm{Log}_{10}T_{1/2}(s)$									
		CYE calculated	CYE (with deformation β_2, P, β_2, D)	CPPMDN [27]	GLDM [25]	ELDM [23]	GLM [26]	EF [24]	GNL [28]	SEB [39]	SHF [40]
^{16}Ne	1.401	–14.47	–	–17.00	–	–16.60	–	–16.16	–	–	–
^{19}Mg	0.75	–10.25	–	–11.99	–	–11.72	–	–10.66	–	–	–
^{22}Si	1.283	–11.79	–8.563	–13.70	–13.30	–13.32	–13.25	–12.30	–13.74	–12.17	–11.78
^{26}S	1.755	–11.99	–11.62	–14.40	–14.59	–13.86	–13.92	–12.71	–14.16	–12.82	–12.93
^{30}Ar	2.28	–12.46	–14.67	–14.99	–	–14.32	–	–13.00	–	–	–
^{34}Ca	1.474	–8.42	–	–10.44	–10.71	–9.92	–10.10	–8.65	–9.93	–8.99	–9.51
^{38}Ti	2.743	–11.97	–	–14.35	–14.27	–13.56	–13.84	–11.93	–13.35	–12.70	–11.77
^{39}Ti	0.758	–0.38	–0.763	–1.23	–1.34	–0.81	–0.91	–0.28	–1.19	–1.91	–1.62
^{42}Cr	1.002	–2.39	–1.632	–2.86	–2.88	–2.43	–2.65	–1.78	–2.76	–2.87	–2.83
^{49}Ni	0.492	13.02	13.024	14.24	14.46	14.64	14.54	12.78	12.43	–	11.05
^{55}Zn	0.48	17.23	18.112	17.66	17.94	–	–	–	–	–	–
^{58}Ge	3.732	–10.23	–11.23	–12.73	–13.10	–11.74	–12.32	–9.53	–10.85	–11.10	–11.06
^{59}Ge	2.102	–4.72	–5.154	–6.99	–6.97	–5.71	–6.31	–4.44	–5.54	–5.41	–5.88
^{60}Ge	0.631	12.24	–	14.00	13.55	14.62	14.24	12.40	12.04	–	12.09
^{64}Se	0.46	24.71	23.551	25.03	24.44	–	–	–	–	–	–

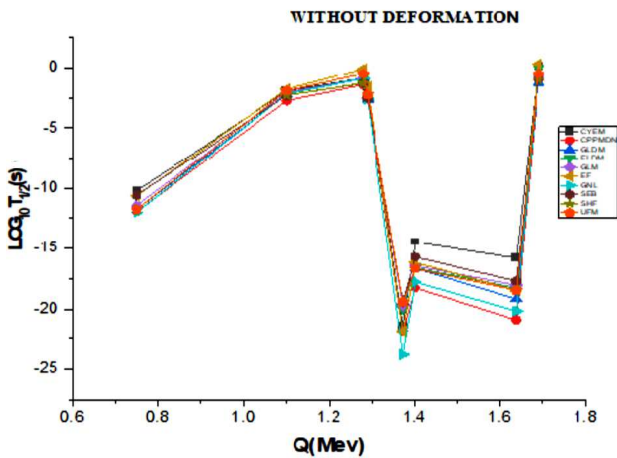**Fig. 1.** Comparision of the predicted 2p radioactivity half lifetimes Using CYE model With available theorectical and experimental value

Fig. 2. Comparision of the predicted 15 even-*Z* nuclei 2p radioactivity half lifetimes using CYE model with available theorectical values without including deformation effects

We expanded the identical research for other even −*Z* nuclei for which 2p radioactivity is energetically possible with energy $Q_{2p} > 0$, and it is shown in Table 3. The calculated results match other forecasted values rather well. The same matches were dis-
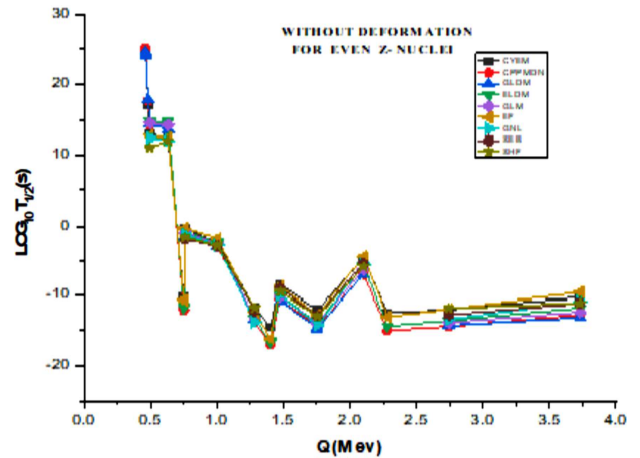
covered in Table 4 as well. The half lifetime value changes when the *Q* value fluctuates slightly. This shows that the half life value depends on the *Q*-value. In Tables 2–4, the impact of the parent and daughter's quadrupole deformation ($\beta2$) are taken

Table 4. **Comparison between the predicted half-lives for various nuclei by using CYE model with and without including deformation effects. The experimental Q_{2p} values and the values of UFM,GLDM and ELDM taken from ref [41] and CPPMDN from ref [50]**

| Parent nuclei	Q_{2p} (MeV)	$\text{Log}_{10}T_{1/2}(s)$					
		CYE	CYE (with deformation β_2, P, β_2, D)	CPPMDN	UFM	GLDM	ELDM
^{5}Be	7.63	−63.69	−	−	−20.58	−	−
^{6}B	7.42	−53.34	−	−	−20.41	−	−
^{7}B	1.42	−18.33	−	−	−19.33	−	−19.19
^{8}C	2.11	−19.03	−	−	−19.80	−	−19.26
^{11}O	4.25	−23.65	−	−	−19.67	−	−19.67
^{13}F	3.09	−17.37	−	−	−19.33	−	−18.89
^{14}F	0.05	8.56	−	12.62	12.22	−	12.31
^{15}Ne	2.52	−15.55	−	−	−18.57	−18.48	−18.08
^{17}Na	3.57	−16.43	−	−	−18.95	−	−18.63
^{22}Si	1.58	−15.55	−13.24	−14.99	−14.61	−18.87	−14.15
^{24}P	1.24	−10.58	−8.928	−10.24	−8.50	−9.41	−8.44
^{26}S	2.36	−16.43	−12.56	−16.19	−16.09	−19.64	−15.15
^{28}Cl	2.72	−13.65	−15.42	−16.35	−15.29	−15.66	−14.49
^{29}Cl	0.10	23.72	−	29.62	28.91	−	29.44
^{29}Ar	5.90	−18.51	−	−	−18.99	−	−18.35
^{30}Ar	3.42	−16.82	−16.32	−17.35	−17.02	−19.66	−16.15
^{32}K	2.74	−13.05	−13.31	−15.61	−14.44	−14.78	−13.68
^{33}Ca	5.13	−17.34	−	−	−18.11	−18.48	−17.35
^{34}Ca	2.51	−12.18	−12.65	−14.65	−14.46	−14.78	−13.56
^{35}Sc	4.98	−14.16	−	−17.36	−16.10	16.63	−15.57
^{37}Sc	0.38	6.92	−	9.72	10.92	10.10	−10.97
^{37}Ti	5.40	−14.12	−	−	−17.81	−17.96	−17.07
^{38}Ti	3.24	−13.66	−12.53	−15.51	−15.18	−15.38	−14.30
^{39}Ti	1.06	−3.67	−3.215	−5.44	−5.41	−5.55	−4.64
^{39}V	4.21	−15.65	−13.84	−16.74	−16.34	−16.54	−15.49
^{40}V	2.14	−10.49	−8.772	−11.87	−11.66	−11.80	−10.80
^{41}Cr	3.33	−12.17	−11.31	−14.87	−14.53	−14.72	−13.66
^{42}Cr	1.48	−5.67	−7.102	−7.60	−7.40	−7.56	−6.66
^{43}Mn	2.48	−10.14	−	−11.91	−10.65	−11.03	−10.16
^{44}Mn	0.50	8.79	−	9.19	9.80	9.51	10.22
^{47}Co	1.02	0.94	0.52	0.11	1.13	0.63	1.37
^{49}Ni	1.08	0.92	0.505	−0.59	0.23	−0.08	0.67
^{52}Cu	1.13	1.09	0.935	1.54	3.45	2.70	3.34
^{55}Zn	0.78	8.29	9.137	7.71	8.77	8.26	8.92
^{56}Ga	2.82	−8.18	−8.727	−11.03	−10.30	−10.83	−9.14
^{57}Ga	1.65	−2.16	−	−3.73	−3.01	−3.81	−2.20
^{58}Ga	0.51	17.09	−	18.27	18.71	17.88	19.33
^{58}Ge	3.23	−9.47	−10.88	−12.00	−11.19	−11.73	−10.02
^{59}Ge	1.60	−1.29	−2.089	−3.23	−2.73	−3.37	−1.76
^{60}As	3.32	−9.45	−10.04	−9.83	−8.37	−9.34	−7.81
^{61}As	1.98	−3.19	−2.55	−5.55	−4.95	−5.61	−3.97
^{62}As	0.59	15.72	15.14	17.51	17.99	17.14	18.58
^{63}Se	2.36	−5.33	−	−7.26	−6.59	−7.22	−5.60
^{64}Se	0.70	12.90	−	14.15	14.39	13.69	15.14
^{65}Br	2.43	−5.155	−	−6.42	−5.55	−6.37	−4.76
^{66}Br	1.39	2.69	−	1.36	1.83	1.12	2.68
^{68}Kr	1.46	2.52	0.740	1.34	1.83	1.13	2.65
^{81}Mo	0.73	21.80	−	22.98	23.26	22.67	23.82
^{85}Ru	1.13	13.84	−	13.67	14.08	13.76	14.66
^{108}Xe	1.01	24.68	−	26.64	27.07	26.37	27.47

a

b
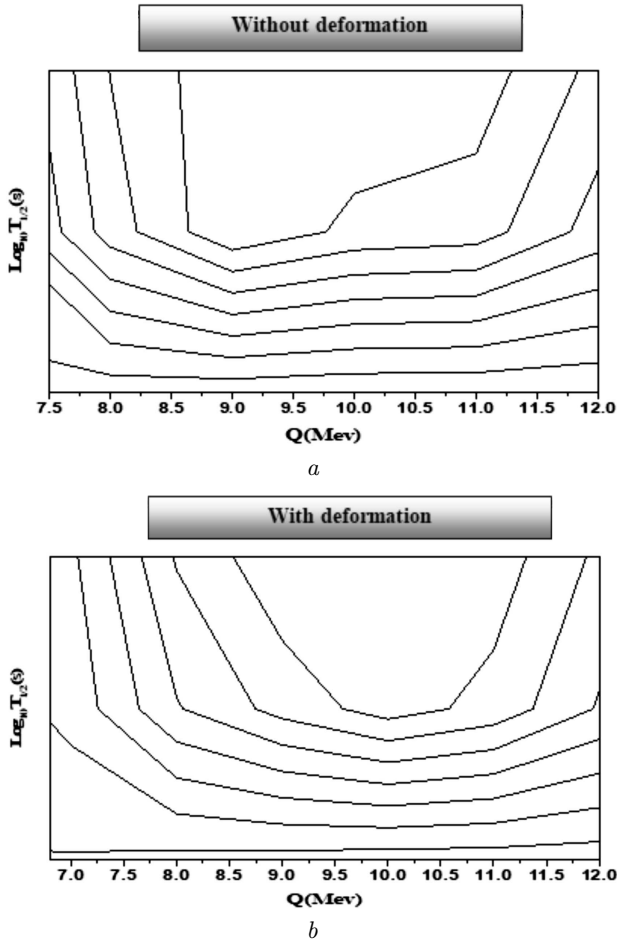
Fig. 3. Forecasts the contour plot of half lifetime values using the CYE model with and without incorporating deformation effects

Fig. 4. Shows the linear relationship between $Q^{-1/2}$, $\mathrm{MeV}^{-1/2}$ and $\mathrm{Log}_{10}T_{1/2}(s)$

Table 5. **To analyze the deviation of the experimental half lifetimes from the calculated ones**

Parent nuclei	Expt. [12, 13]	CYEM calculated	$\log_{10}\mathrm{HF} = (\mathrm{CYEM})$ $\log_{10}T_{1/2}^{\exp} - \log_{10}T_{1/2}^{\mathrm{CYEM}}$
^{6}Be	$-20.30^{+0.03}_{-0.03}$	-21.41	1.11
^{16}Ne	$-20.38^{+0.03}_{-0.03}$	-14.47	-5.91
^{19}Mg	$-11.40^{+0.14}_{-0.20}$	-10.25	-1.15
^{45}Fe	$-2.40^{+0.26}_{-0.26}$	-1.94	-0.46
^{48}Ni	$-2.52^{+0.24}_{-0.22}$	-1.67	-0.85
^{54}Zn	$-2.76^{+0.15}_{-0.14}$	-0.9	-1.86
^{67}Kr	$-1.70^{+0.02}_{-0.02}$	0.11	-1.81

into account. The deformation values were obtained from the mass tables of Möller *et al.* [49]. The inclusion of deformation effects decreases the half life-time values, because the height and width of the barrier are reduced, and the structure is altered by the addition of deformation effects in both the parent and daughter nuclei (β_{2p}, β_{2D}). The values were raised in some instances. In order to find the value of logarithm hindrance factor $\log_{10}\mathrm{HF}$), the deviation of the experimental from calculated ones $\log_{10}\mathrm{HF} = \log_{10}T_{1/2}^{\exp} - \log_{10}T_{1/2}^{\mathrm{CYEM}}$, Table 5 displays this statistics. The Table shows that the cases of ^{19}Mg, ^{6}Be, ^{54}Zn and ^{67}Kr most values of $\log_{10}\mathrm{HF}$ are between –1 and 1. CYE shows equivalent accuracy to the other models, when the half lifetimes are compared.
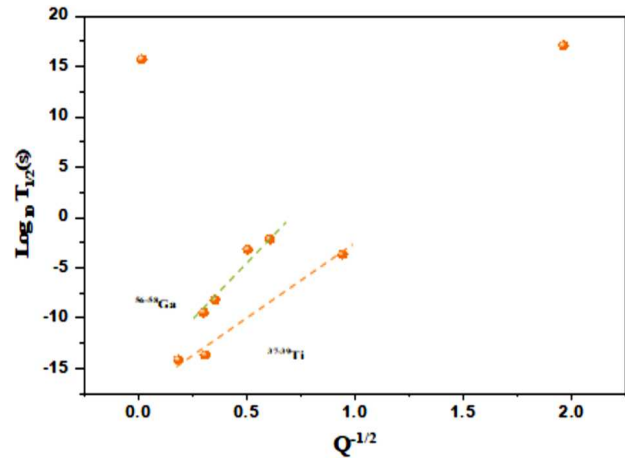
Fig. 1 and 2 shows the variation of half life time values with Q value for 2p radioactivity. Here, the CYEM predictions and the CPPMDN, GLDM values diverge significantly, while the EF deviation is minimal. To explore the variations in half-life time values for two proton elements without and with adding the result of deformation, the contours depicted in Figs. 3, *a* and 3, *b* were created. Contour lines are mix of straight and curved lines. Comparing Fig. 3, *b*'s closed contours to the contour plot of half lifetime values in 3, *a*, the closed contours are significantly shorter and when they get closer to the boundary, they get more like straight lines. This suggests that, as a result of the parent nucleus' deformation, the daughter nucleus' stability rises. The $G - N$ graphs between the quantity $\mathrm{Log}_{10}T_{1/2}(s)$ and

$Q^{-1/2}$ (Mev)$^{-1/2}$ for the 2p emission from parent nuclei $^{37-39}$Ti, $^{56-58}$Ga are shown in Fig. 4. The elements are chosen at random. It seemingly linear behavior exists. As a result, we can say that two-proton radioactivity abides under the $G - N$ law.

6. Summary and Conclusion

The two proton radioactive half lifetimes are explored in this work for the parent nuclei ^{6}Be, ^{12}O, ^{16}Ne, ^{19}Mg, ^{45}Fe, ^{48}Ni, ^{54}Zn, ^{67}Kr and other even $Z \geq 4$ to $Z \leq 54$ parent nuclei in the range emitting proton pair using CYE model in the two sphere approximation and including deformation effects. The results obtained are contrasted with the other two empirical formulas and six other theoretical models. Additionally, the results are in accordance with prior predictions. We anticipate that the lengthened half lifetimes of these forecasted nuclei will aid future experimental studies of two proton decay.

1. Y.B. Zel'dovich. The existence of new isotopes of light nuclei and the equation of state of neutrons. *Sov. Phys. JETP* **11**, 812 (1960).
2. V.I. Goldansky. On neutron-deficient isotopes of light nuclei and the phenomena of proton and two-proton radioactivity. *Nucl. Phys.* **19**, 482 (1960).
3. G.J. KeKelis, M.S. Zisman, D.K. Scott, R. Jahn, D.J. Vieira, Joseph Cerny, F. Ajzenberg-Selove. Masses of the unbound nuclei ^{16}Ne, ^{15}F and ^{12}O. *Phys. Rev. C* **17**, 1929 (1978).
4. O.V. Bochkarev, A.A. Korsheninnikov, E.A. Kuz'min, I.G. Mukha, A.A. Ogloblin, L.V. Chulkov, G.B. Yan'kov. Two-proton decay of ^{6}Be. *JETP Lett.* **40**, 969 (1984).
5. B.A. Brown. Diproton decay of nuclei on the proton drip line. *Phys. Rev. C* **43**, R1513 (1991).
6. C.R. Bain, P.J. Woods, R. Coszach, T. Davinson, P. Decrock, M. Gaelens, W. Galster, M. Huyse, R.J. Irvine, P. Leleux, E. Lienard, M. Loiselet, C. Mi-chotte, R. Neal, A. Ninane, G. Ryckewaert *et al.* Two proton emission induced via a resonance reaction. *Phys. Lett. B* **373**, 35 (1996).
7. M.J. Chromik, B.A. Brown, M. Fauerbach, T. Glasmacher, R. Ibbotson, H. Scheit, M. Thoennessen, P.G. Thirolf. Excitation and decay of the first excited state of ^{17}Ne. *Phys. Rev. C* **55**, 1676 (1997).
8. I. Mukha, G. Schrieder. Two-proton radioactivity as a genuine three-body decay: The ^{19}Mg probe. *Nucl. Phys. A* **690**, 280 (2001).
9. M. Pfützner, E. Badura, C. Bingham, B. Blank, M. Chartier, H. Geissel, J. Giovinazzo, L.V. Grigorenko, R. Grzywacz, M. Hellström. First evidence for the two-proton decay of ^{45}Fe. *Eur. Phys. J. A* **14**, 279 (2002).
10. J. Giovinazzo, B. Blank, M. Chartier, S. Czajkowski, A. Fleury, M.J. Lopez Jimenez, M.S. Praviko, J.C. Thomas, F. de Oliveira Santos, M. Lewitowicz, V. Maslov, M. Stanoiu, R. Grzywacz, M. Pftzner *et al.* Two-proton radioactivity of ^{45}Fe. *Phys. Rev. Lett.* **89**, 102501 (2002).
11. B. Blank *et al.* First observation of ^{54}Zn and its decay by two-proton emission. *Phys. Rev. Lett.* **94**, 232501 (2005).
12. I. Mukha, E. Roeckl, L. Batist, A. Blazhev, J. Doring, H. Grawe, L. Grigorenko, M. Huyse, Z. Janas, R. Kirchner, M. La Commara, Ch. Mazzocchi, Sam L. Tabor, Piet Van Duppen. Proton-proton correletions observed in two proton radioactivity of ^{94}Ag. *Nature* **439**, 298 (2006).
13. J. Rotureau, J. Okołowicz, M. Płoszajczak. Theory of the two-proton radioactivity in the continuum shell model. *Nucl. Phys. A* **767**, 13 (2006).
14. I. Mukha, K. Sümmerer, L. Acosta, M.A.G. Alvarez, E. Casarejos, A. Chatillon, D. Cortina-Gil, J. Espino, A. Fomichev, J.E. García-Ramos, H. Geissel, J. Gómez-Camacho, L. Grigorenko, J. Hoffmann, O. Kiselev *et al.* Observation of two- proton radioactivity of ^{19}Mg by tracking the decay products. *Phys. Rev. Lett.* **99**, 182501 (2007).
15. J. Giovinazzo *et al.* First direct observation of two protons in the decay of ^{45}Fe with a time-projection chamber. *Phys. Rev. Lett.* **99**, 102501 (2007).
16. K. Miernik *et al.* Studies of charged particle emission in the decay of ^{45}Fe. *Acta Phys. Polonica B* **39**, 477 (2008).
17. I. Mukha, L. Grigorenko, K. Sümmerer, L. Acosta, M.A. G. Alvarez, E. Casarejos, A. Chatillon, D. Cortina-Gil, J.M. Espino, A. Fomichev, J.E. García-Ramos, H. Geissel, J. Gómez-Camacho, J. Hofmann, O. Kiselev *et al.* Proton-proton correlations observed in two-proton decay of ^{19}Mg and ^{16}Ne. *Phys. Rev. C* **77**, 061303(R) (2008).
18. L.V. Grigorenko. Theoretical study of two-proton radioactivity. Status, predictions, and applications. *Phys. Part. Nucl.* **40**, 674 (2009).
19. M.F. Jager, R.J. Charity, J.M. Elson, J. Manfredi, M.H. Mahzoon, L.G. Sobotka, M. McCleskey, R.G. Pizzone, B.T. Roeder, A. Spiridon, E. Simmons, L. Trache, M. Kurokawa. Two-proton decay of ^{12}O and its isobaric analog state in ^{12}N. *Phys. Rev. C* **86**, 011304 (2012).
20. K.W. Brown, R.J. Charity, L.G. Sobotka, Z. Chajecki, L.V. Grigorenko, I.A. Egorova, Yu.L. Parfenova, M.V. Zhukov, S. Bedoor, W.W. Buhro, J.M. Elson, W.G. Lynch, J. Manfredi, D.G. McNeel, W. Reviol *et al.* Observation of long- range three-body coulomb effects in the decay of ^{16}Ne. *Phys. Rev. Lett.* **113**, 232501 (2014).
21. T. Goigoux, P. Ascher, B. Blank, M. Gerbaux, J. Giovinazzo, S. Grévy, T. Kurtukian Nieto, C. Magron, P. Doornenbal, G.G. Kiss, S. Nishimura, P.A. Söderström, V.H. Phong, J. Wu, D.S. Ahn *et al.* Two-proton radioactivity of ^{67}Kr. *Phys. Rev. Lett.* **117**, 162501 (2016).
22. T.B. Webb *et al.* First observation of unbound ^{11}O, the mirror of the halo nucleus ^{11}Li. *Phys. Rev. Lett.* **122**, 122501 (2019).
23. M. Gonalves, N. Teruya, O.A.P. Tavares, S.B. Duarte. Two-proton emission half-lives in the effective liquid drop model. *Phys. Lett. B* **774**, 14 (2017).
24. I. Sreej, M. Balasubramaniam. An empirical formula for the half-lives of exotic two-proton emession. *Eur. Phys. J. A* **55**, 33 (2019).

25. J.P. Cui, Y.H. Gao, Y.Z. Wang *et al.* Two-proton radioactivity within a generalized liquid drop model. *Phys. Rev. C* **101**, 014301 (2020).

26. H.M. Liu, Y.T. Zou, X. Pan, You-Tian Zou, Jiu-Long Chen, Jun-Hao Cheng, Biao He, Xiao-Hua Li. Systematic study of two-proton radioactivity within a Gamow-like model. *Chin. Phys. C* **45**, 044110 (2021).

27. K.P. Santhosh. Theoretical studies on two-proton radioactivity. *Phys. Rev. C* **104**, 064613 (2021).

28. H.M. Liu, Y.T. Zou, X. Pan, De-Xing Zhu, Yang-Yang Xu, Xi-Jun Wu, Peng-Cheng Chu, Xiao-Hua Li. New Geiger-Nuttall law for two-proton radioactivity. *Chin. Phys. C* **45**, 024108 (2021).

29. G. Shanmugam, B. Kamalaharan. Exotic decay model and alpha decay studies. *Phys. Rev. C* **41**, 1742 (1990).

30. G. Shanmugam, G.M. Carmel Vigila Bai, B. Kamalaharan. Cluster radioactivities from an island of cluster emitters. *Phys. Rev. C* **51**, 2616 (1995).

31. G.M. Carmel Vigila Bai, R. Nithya Agnes. Role of multi polarity-six deformation parameter on exotic decay half-life of Berkelium nucleus. *IOSR-J. Appl. Phys.* **17**, 84 (2017).

32. G.M. Carmel Vigila Bai, J. Umai Parvathiy. Alpha decay properties of heavy and superheavy elements Pramana. *J. Phys.* **84** (1), 113 (2015).

33. J. Umai Parvathy. Dr. Sci. thesis. *Properties of Superheavy Elements in Trans-actinide Region* (Manonmanium sundaranar university 2016) (in Tirunelveli).

34. G.M. Carmel Vigila Bai, R. Revathi.Alpha and heavy cluster radioactivity of superheavy nuclei $100 \leq Z \leq 120$. *J. Phys.: Conf. Ser.* **1706**, 012021 (2020).

35. G.M. Carmel Vigila Bai, R. Abisha. Two proton radioactivity of nuclei – $Z \geq 4$ to $Z \leq 36$. In: *Proceedings of the International Conference of IVCARTMSN, May 24* (2022).

36. G.M. Carmel Vigila Bai, R. Abisha. Two proton Radioactivity of nuclei – $Z \geq 4$ to $Z \leq 54$. In: *Proceedings of the National Seminar on Functional Materials and Its Application NSFMA October 14* (2022) [ISBN: 978-93-84737-37-5].

37. G.M. Carmel Vigila Bai, R. Abisha. Two proton radioactivity of heavy and super heavy mass region – $Z \geq 100$ to $Z \leq 111$. In: *Proceedings of the International Conference on Interdisciplinary Research in Chemistry ICIRC'23, February 24–25* (2023) [ISBN: 978-93-5812-971-7].

38. G.M. Carmel Vigila Bai. Dr. Sci., thesis. *A Systematic Study of Cluster Radioactivity in Trans-tin region* (Manonmanium sundaranar university, 1997).

39. You-Tian Zou, Xiao Pan, Xiao-Hua Li, Hong-Ming Liu, Xi-Jun Wu, Biao He. Systematic study of two-proton radioactivity with a screened electrostatic barrier. *Chin. Phys. C* **45**, 104102 (2021).

40. Xiao Pan, You-Tian Zou, Hong-Ming Liu, Biao He, Xiao-Hua Li, Xi-Jun Wu, Zhen Zhang. Systematic study of two-proton radioactivity half-lives using the two-potential and Skyrme–Hartree–Fock approaches. *Chin. Phys. C* **45**, 124104 (2021).

41. F. Xing, J. Cui, Y. Wang, J. Gu. Two-proton radioactivity of ground and excited states within a unified fission model. *Chin. Phys. C* **45**, 124105 (2021).

42. W. Whaling. Magnetic analysis of the $Li^6(He^3, t)Be^6$ reaction. *Phys. Rev.* **150**, 836 (1966).

43. C.J. Woodward, R.E Tribble, D.M. Tanner. Mass of ^{16}Ne. *Phys. Rev. C* **27**, 27 (1983).

44. M. Pomorski, M. Pfützner, W. Dominik, R. Grzywacz, A. Stolz, T. Baumann, J.S. Berryman, H. Czyrkowski, R. Dabrowski, A. FIjalkowska, T. Ginter, J. Johnson, G. Kaminski, N. Larson, S.N. Liddick *et al.* Proton spectroscopy of ^{48}Ni, ^{46}Fe, and ^{44}Cr. *Phys. Rev. C* **90**, 014311 (2014).

45. P. Ascher, L. Audirac, N. Adimi, B. Blank, C. Borcea, B.A. Brown, I. Companis, F. Delalee, C.E. Demonchy, F. de Oliveira Santos, J. Giovinazzo, S. Grevy, L.V. Grigorenko, T. Kurtukian-Nieto, S. Leblanc *et al.* Direct observation of two protons in the decay of ^{54}Zn. *Phys. Rev. Lett.* **107**, 102502 (2011).

46. C. Dossat, A. Bey, B. Blank, G. Canchel, A. Fleury, J. Glovinazzo, I. Matea, F. de Oliveira Santos, G. Georgiev, S. Grevy, I. Stefan, J.C. Thomas, N. Adimi, C. Borcea, D. Cotina Gil *et al.* Two-proton radioactivity studies with ^{45}Fe and ^{48}Ni. *Phys. Rev. C* **72**, 054315 (2005).

47. L. Audirac, P. Ascher, B. Blank, C. Borcea, B.A. Brown, G. Canchel, C.E. Demonchy, F. de Oliveira Santos, C. Dossat, J. Gio Vinazzo, S. Grevy, L. Hay, J. Huikari, S. Leablanc, I. Matea *et al.* Direct and β-delayed multi-proton emession from atomic nuclei with a time projection chamber: The cases of ^{43}Cr, ^{45}Fe and ^{51}Ni. *Eur. Phys. J. A* **89**, 102501 (2002).

48. M. Wang, G. Audi, F.G. Kondev, W.J. Huang, S. Naimi, Xing Xu. The Ame2016 atomic mass evaluation. (II). Tables, graphs and references. *Chin. Phys. C* **41**, 030003 (2017).

49. P. Möller, A.J. Sierk, T. Ichikawa, H. Sagawa. Nuclear ground-state masses and deformations: FRDM (2012). *At. Data Nucl. Data* Tables I **109**, 1 (2016).

50. K.P. Santhosh. Two-proton radioactivity within a coulomb and proximity potential model for deformed nuclei. *Phys. Rev. C* **106**, 054604 (2022).

Г.М. Кармел Віджіла Бай, Р. Абіша

МОЖЛИВА ДВОПРОТОННА ЕМІСІЯ
З ЯДЕР В ОБЛАСТІ $4 \leq Z \leq 54$ НА ОСНОВІ
МОДИФІКОВАНОЇ CYE МОДЕЛІ

Двопротонна радіоактивність – це спонтанна емісія одночасно двох протонів із ядра. В цій роботі ми узагальнили нашу CYE модель для розгляду 2p радіоактивності ядер від $Z \geq 4$ до $Z \leq 54$ з урахуванням деформації ядра. Наші результати, отримані на базі CYE моделі, добре узгоджуються з іншими теоретичними моделями.

К л ю ч о в і с л о в а: двопротонна радіоактивність, CYE модель, період напіврозпаду, ефекти деформації.